



Berg Huettenmaenn Monatsh (2022) Vol. 167 (12): 566–577
<https://doi.org/10.1007/s00501-022-01304-5>
 © The Author(s) 2022

BHM Berg- und
Hüttenmännische
Monatshefte

Comparative Analysis of Numerical Methods Regarding the Backflow Investigation in Tunnels of Zentrum am Berg

Aliaksei Patsekha, Ranzhu Wei, and Robert Galler

Chair of Subsurface Engineering, Montanuniversität Leoben, Leoben, Austria

Received October 28, 2022; accepted October 31, 2022; published online December 2, 2022

Abstract: The efficiency of tunnel ventilation systems is commonly evaluated through numerical modelling. In this survey, two CFD models were developed by means of Fire Dynamic Simulator and Ansys Fluent software. The simulation results were used to assess the model performance in studying the backflow distribution in a real tunnel. A full-scale experiment to evaluate the ventilation conditions in the western railway tunnel was carried out in Zentrum am Berg. The velocity values were obtained for 90 examined points located at 10 cross-sections along a 100-meter tunnel part. The results showed good agreement in velocity variation trends from field measurements and those predicted by numerical models. At cross-sections more distant from the fan outlets, the FDS and Fluent models overestimated the flow velocities to a different extent. The simulated backflow development corresponds well to the observed three specified regions (initial, transitional, and developed) with distinctive flow structures. The FDS calculations confirmed the registered spontaneous changes in flow direction at points with a prevailed flow direction in the vicinity of the jet fans. Despite some discrepancies in results, the comparative analysis of two numerical models showed their applicability in the backflow investigation.

Keywords: Tunnel ventilation, Numerical simulation, Full-scale experiment, Backflow investigation

Vergleichende Analyse numerischer Methoden zur Rückstauuntersuchung in Tunneln des Zentrums am Berg

Zusammenfassung: Die Effizienz von Tunnellüftungssystemen wird in der Regel durch numerische Modellierung bewertet. In dieser Studie wurden zwei CFD-Modelle mit Hilfe des Fire Dynamic Simulators und der Software Ansys

Fluent entwickelt. Die Simulationsergebnisse wurden verwendet, um die Leistung des Modells bei der Untersuchung der Rückströmungsverteilung in einem realen Tunnel zu bewerten. Im Zentrum am Berg wurde ein großmaßstäbliches Experiment zur Bewertung der Lüftungsbedingungen im westlichen Eisenbahntunnel durchgeführt. Die Geschwindigkeitswerte wurden für 90 untersuchte Punkte an 10 Querschnitten entlang eines 100 m langen Tunnelabschnitts ermittelt. Die Ergebnisse zeigten eine gute Übereinstimmung zwischen den Trends der Geschwindigkeitsvariationen aus den Feldmessungen und denen, die von den numerischen Modellen vorhergesagt wurden. An weiter entfernten Querschnitten von den Ventilatorauslässen überschätzten die Modelle FDS und Fluent die Strömungsgeschwindigkeiten in unterschiedlichem Maße. Die simulierte Rückflussentwicklung entspricht gut den beobachteten drei festgelegten Regionen (Anfangs-, Übergangs- und Entwicklungsbereich) mit ausgeprägten Strömungsstrukturen. Die FDS-Berechnungen bestätigten die beobachteten spontanen Änderungen der Strömungsrichtung an Stellen mit einer vorherrschenden Strömungsrichtung in der Nähe der Strahlfächer. Trotz einiger Diskrepanzen in den Ergebnissen

zeigte die vergleichende Analyse der beiden numerischen Modelle ihre Anwendbarkeit bei der Untersuchung der Rückströmung.

Schlüsselwörter: Tunnelbelüftung, Numerische Simulation, Experiment im Originalmaßstab, Rückflussuntersuchung

1. Introduction

Safe tunnel construction and operation is a key challenge in a wide range of engineering disciplines as the safety and comfort of the people remain the priority in various conditions. During tunnel construction, the detonation of explosives and the use of diesel engines generate toxic emissions that can seriously endanger the health and safety of construction workers. Road tunnel ventilation systems aim to limit the concentration of air pollutants under normal

A. Patsekha, Inž.-Mech. Ktn (✉)
 Chair of Subsurface Engineering,
 Montanuniversität Leoben,
 Erzherzog-Johann Straße 3,
 8700 Leoben, Austria
aliaksei.patsekha@unileoben.ac.at

tunnel operation providing fresh air and then removing the exhaust fumes from the tunnel. And, of course, ventilation is the most common measure to mitigate fire effects and remove smoke, heat, and contaminants from tunnels [1].

The dynamically changing environment, techniques, and machinery constantly produce new challenges for researchers in the area of tunnel ventilation. Computational fluid dynamics (CFD) provides effective solutions to a wide range of problems in many fields of study and industries, including aerodynamics, fluid dynamics, heat transfer, environmental engineering, and industrial system design and analysis. As of today, computer numerical simulations are integral for studying the efficiency of multiple engineering methods due to a cost-effective approach and available amount of data [2].

Recent research shows great value in the use of CFD models in assessing tunnel ventilation objectives under diverse scenarios [3–7]. A variety of CFD software packages is available to resolve the whole range of emerging issues, whereas Ansys Fluent is the most used fluid flow simulation module [8]. Fire Dynamics Simulator (FDS) is an alternative open-source CFD program designed to deal with problems in the field of fluid dynamics and heat transfer.

Ansys Fluent is a general-purpose CFD software that contains comprehensive modelling capabilities needed to model fluid flow, turbulence, heat and mass transfer, and reactions for industrial applications. This program is based on a finite volume method and solves the partial differential equations that define the energy, mass, and momentum conservation. Thus, Fluent converts the general transport equations to a system of linear equations that are solved numerically by a point implicit (Gauss-Seidel) algorithm in conjunction with an algebraic multigrid (AMG) method [9]. The availability of the different turbulence models, e.g. Reynolds Time-Averaged Navier-Stokes Equations (RANS), Large Eddy Simulation (LES) and others allows studying general questions of aerodynamics phenomena and occasionally occurring tasks such as optimization of tunnel ventilation systems.

Ansys Fluent is commonly applied for numerical simulations and further analysis of tunnel ventilation operations because of the enhanced possibility of geometry modelling and available physical models [10]. Theoretical and experimental results were obtained for various tunnel operation scenarios where the airflow of jet fans and ventilation ducts was simulated and validated by field measurements providing the background for optimization recommendations [11–15].

The second program used in the area under discussion is Fire Dynamics Simulator. It is a computational fluid dynamics model that solves numerically a form of the Navier-Stokes equations appropriate for low-speed, thermally-driven flow with an emphasis on smoke and heat transport from fires [16]. FDS is a large eddy simulation (LES) model that uses an explicit second-order predictor/corrector scheme within the Cartesian coordinate system where the turbulent viscosity is obtained from the Deardorff eddy viscosity model. All the details of the FDS mathematical model are comprehensively described in the FDS Technical Reference Guide (Volume 1) [17].

Despite the initially indicated purpose, this forensic tool was gradually improved, and now it can be successfully applied to analyse different fluid dynamics problems of various complexity. Several FDS models with a focus on ventilation issues in tunnels are evaluated within the verification and validation procedures and given in the FDS Technical Reference Guide (Volumes 2 and 3) [18, 19], acknowledging the possibility of obtaining reliable and accurate results. Furthermore, many examples of the FDS model implementation in the design and performance assessment of ventilation and air conditioning systems, optimization of tunnel ventilation and other areas have been published in academic journals or presented at scientific conferences [20–22]. The relatively limited adoption of FDS in tunnel applications is largely due to the requirement of a rectilinear mesh whereas other CFD modules may support unstructured grids to better reflect the actual tunnel structure. However, studies show that even in the case of replacing the original arch-shaped tunnel cross-section with a rectangular one, it is possible to obtain results with sufficient accuracy by taking into consideration the corresponding hydraulic (equivalent) diameter [23, 24].

Reverse or backflow is a feature of jet fan ventilation that requires special attention in underground infrastructure systems due to the presence of harmful gases and particulate matter on-site during construction or the generation of combustion products by vehicles under normal tunnel operation, as well as the emergence of heat and smoke in a case of fire [25]. In all cases, harmful contaminants pose a real danger to people and can cause serious health issues and even death, since air backflow is able to prevent the removal of pollutants from the underground space. Recent research is mainly focused on the investigation of backflow features during the tunnel construction phase or in the event of an emergency in an operating tunnel [26, 27]. But there are also a number of studies that review the potential impact of backflow in forced ventilated tunnels [28–31].

Therefore, this study aims to evaluate the performance of the two most popular software packages (Ansys Fluent and FDS) regarding the backflow investigation in the western railway tunnel of the research facility “Zentrum am Berg” by comparing it with experimental observations.

2. Research Approach and Methodology

2.1 Full-scale Experiment

2.1.1 Experimental Setup

The experimental part of the study was conducted at the Zentrum am Berg (ZaB) in Eisenerz, Austria. This facility represents an independent research infrastructure for a wide variety of purposes. It consists of a two-tube road tunnel and two parallel railway tunnel tubes as well as a test tunnel enabling research, development, education, and training under real underground conditions (Fig. 1a).

A series of measurements were carried out in the western railway tunnel (despite the name, there are no railways

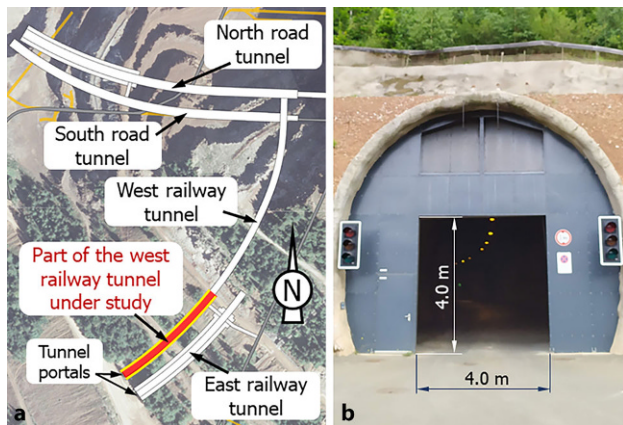


Fig. 1: Tunnel scheme at the Zentrum am Berg (a) and the portal of the western railway tunnel (b)

in the tunnel, and the ground surface represents an asphalt road). The tunnel is slightly curved and has a length of 403 m, a width of 8.27 m, and a height of 7.55 m. Shotcrete is used as a lining for the tunnel walls and ceiling. The considered tunnel section (170 m long) has an elevation of 1084 m a. s. l. Two jet fans are installed on the tunnel ceiling at a distance of 50 m from the tunnel portal. According to the manufacturer’s documentation, the fans are fully reversible and have a nominal diameter of 1.12 m and a length of 3.0 m. The main fan characteristics are given in Table 1.

Air velocity measurements were performed in two stages. The detailed measuring scheme is given in Fig. 2. For clarity and convenience, it is assumed that the fan outlets are positioned at the 0-meter mark. The first phase included the evaluation of the naturally developed flow inside the tunnel. For this reason, the velocity values were measured at different points on several cross-sections within the considered tunnel part, including two outermost cross-sections (NV-U_s and NV-D_s). During the second

TABLE 1 Jet fan parameters		
Parameter	Value	Unit
Thrust	1100	N
Velocity	31.8	m/s
Volume flow	31.4	m ³ /s
Rotational speed	1470	1/min

phase, 10 cross-sections at 10 m to 100 m from the fan outlets (10 m between the adjacent planes) were studied under the operating jet fans. To cover an entire tunnel cross-section, measurements were held for 9 points—3 rows (1, 2, 3) and 3 columns (A, B, C). As a result, air velocity was recorded for 90 points along the 100-meter tunnel section.

The air velocity was recorded by Voltcraft PL-130 AN anemometer. This device is designed to measure the temperature, velocity, and volume flow of gases. Effective velocity (average speed), maximum or minimum speed can also be displayed during the measuring process. The main technical parameters of the anemometer are as follows: air velocity measuring range 0.4 ... 30 m/s, resolution 0.01 m/s, basic accuracy ±3%; temperature measuring range -10 ... +60 °C, resolution 0.1 °C, accuracy 2 °C; working humidity less than 80% RH.

The anemometer was additionally fitted out with a tuft of short flexible paper strips to be used as a flow direction indicator [32]. This helped to observe the backflow development since in turbulent conditions the directional changes occur so quickly that the measuring device (for example, a vane anemometer) is not always capable of recording them.

The pressure measurements were also performed to determine its effect on the development of natural conditions inside the tunnel. For this reason, one point in front of the tunnel entrance (“Ambient” area in Fig. 2) and four points within the first 150 m of the tunnel were assessed. The DP-Calc Micromanometer 5825 was used to estimate the pressure difference between the ambient and tunnel locations. This device has a -3735 to +3735 Pa measuring range with a reading accuracy of ±1% and a resolution of 0.1 Pa.

2.1.2 Experimental Results

The natural ventilation in the ZaB tunnels is defined by the pressure differential between the tunnel portals created by differences in elevation, ambient temperatures and wind. During the tests, the naturally developing airflow was measured at and in between the upstream (NV-U_s) and downstream (NV-D_s) cross-sections (Fig. 2). The majority of results were in the range between 0 and 0.5 m/s. This low (under 0.4 m/s on average) natural flow was directed inside the tunnel (similar to the direction of the flow from the operating fans) and can be mostly explained by the favourable ambient conditions (partly cloudy, southeast wind under 6 km/h).

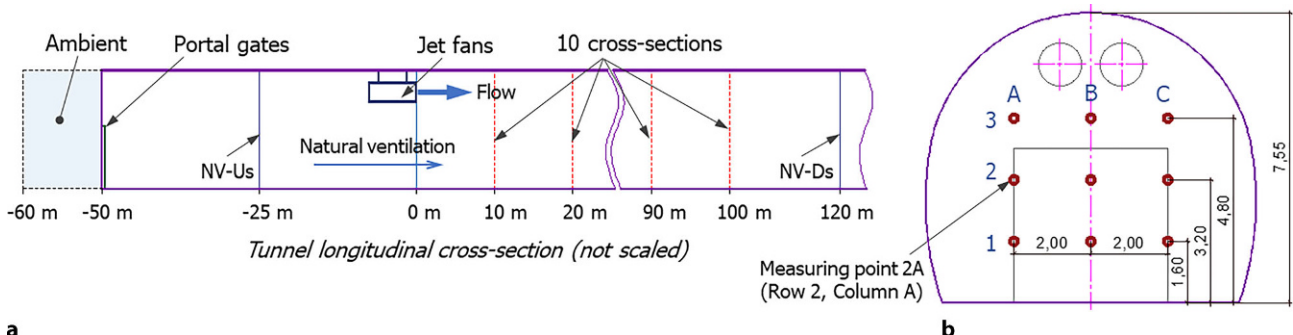


Fig. 2: Overlay of the tunnel (a) and the arrangement of measuring points at each cross-section (b)

The main measuring session started after the fans were switched on and the air flow inside the tunnel became quasi-stable. During the measurements, three areas with distinctive flow structures were observed.

The first “initial” region (0 ... ~40 m) is characterised by the non-uniformity of the airflow, vortices, and constant directional changes of the local airstreams. An extremely turbulent vortex area is formed in the immediate vicinity (0 ... ~20 m) of the fans. The backflow presence in the first zone was repeatedly confirmed by the observations.

The second “transitional” region (~40 ... ~60 m) represents a transition area where the air flow is more balanced though high magnitude fluctuations appear recurrently. Negative velocity values indicating the backflow existence were monitored occasionally.

In the third “developed” region (~60 ... ~100 m), the flow velocity gradually decreases, and the flow field distribution tends to be stable and uniform.

Preliminary tests showed a big difference in measured velocity values during a 3-minute spell at the first and the second regions due to the flow complexity. For this reason and considering the sequenced measurements, it was

decided to record maximal and minimal values of air velocity at every point during the 30s period. It allowed us to establish the velocity ranges for every measuring point and analyse the backflow development. The experimental results of full-scale ventilation tests are given in Table 2.

The points from the same row (1, 2, or 3) have a sufficiently identical pattern, especially when considering areas limited by the maximum-minimum lines. Negative and positive velocities denote the flow direction. The flow generated by the fans as well as the naturally developed airflow is assumed to be positive, while the backflow gusts are defined as negative. The cells with values in italics and bold in Table 2 indicate the flow directions observed with the marker technique during the tests.

Air velocities were also measured at four points (locations similar to A1, B1, B2, and C1) at the “NV-Us” cross-section (~25 m) to provide data on the flow behaviour in the upstream part of the tunnel. The obtained results are given in Table 3.

Air temperature (with an average value of 11.5°C) inside the tunnel was also recorded during the tests.

TABLE 2
Measured ventilation velocities in the tunnel

Point	Velocity, m/s	Position of a cross-section, m									
		10	20	30	40	50	60	70	80	90	100
A1	Maximum	<i>-0.11</i>	2.10	5.42	6.58	2.66	2.68	1.77	1.51	1.58	1.60
	Average	-2.02	-2.01	1.77	2.56	2.07	1.77	1.27	1.18	1.25	1.43
	Minimum	-5.42	-5.19	-1.50	1.43	1.27	1.13	0.88	0.91	1.04	1.20
A2	Maximum	<i>-0.11</i>	2.20	8.70	5.98	3.88	2.02	1.68	1.81	1.64	1.60
	Average	-1.83	-2.08	4.12	3.71	1.64	1.53	1.41	1.43	1.51	1.43
	Minimum	-4.38	-4.42	0.85	1.62	1.05	1.04	1.04	1.08	1.18	1.25
A3	Maximum	12.48	10.76	10.46	5.47	1.56	2.33	1.96	1.73	1.79	1.79
	Average	7.48	7.48	6.45	3.43	1.10	1.39	1.66	1.39	1.48	1.58
	Minimum	1.81	4.31	2.37	0.66	0.60	0.63	1.25	0.99	1.00	1.25
B1	Maximum	<i>-1.29</i>	<i>-0.38</i>	3.76	4.41	2.52	1.79	1.68	1.29	1.47	1.60
	Average	-2.15	-3.59	1.66	1.89	2.00	1.51	1.34	1.10	1.20	1.41
	Minimum	-4.68	-6.40	-3.50	0.13	1.13	1.27	0.82	1.02	1.03	1.18
B2	Maximum	<i>-1.29</i>	<i>-0.30</i>	4.93	3.81	2.62	2.01	1.58	1.43	1.60	1.47
	Average	-2.52	-2.09	1.58	1.89	1.60	1.58	1.32	1.18	1.36	1.43
	Minimum	-4.54	-4.96	-2.20	0.08	0.93	1.15	0.99	1.07	1.03	1.18
B3	Maximum	10.12	9.70	6.94	6.19	1.98	2.23	1.98	1.58	1.46	1.49
	Average	5.10	6.59	3.59	1.77	1.48	1.62	1.53	1.32	1.29	1.36
	Minimum	1.68	1.13	1.53	0.08	0.41	1.03	0.96	1.10	1.15	1.05
C1	Maximum	<i>-0.22</i>	<i>-2.11</i>	3.50	3.90	2.23	1.94	1.54	1.51	1.60	1.43
	Average	-2.43	-4.26	1.94	1.85	1.73	1.27	1.34	1.39	1.25	1.20
	Minimum	-5.70	-5.66	-2.50	0.69	1.20	0.71	1.13	1.18	1.03	1.07
C2	Maximum	<i>-1.62</i>	<i>-1.20</i>	6.48	2.41	2.11	2.54	1.73	1.56	1.51	1.54
	Average	-2.68	-2.46	2.08	1.15	1.58	1.66	1.60	1.43	1.34	1.34
	Minimum	-5.24	-4.68	-2.60	-0.80	1.29	1.43	1.22	1.20	1.15	1.13
C3	Maximum	7.32	5.98	7.41	2.08	1.92	2.19	2.06	1.92	1.66	1.68
	Average	2.35	2.58	2.56	0.96	1.27	1.60	1.60	1.49	1.58	1.51
	Minimum	0.30	0.19	-2.50	0.22	0.66	1.41	1.46	1.10	1.32	1.22

italics—positive flow direction was observed
bold—negative flow direction was observed

TABLE 3
Measured air velocities at the upstream cross-section

Point	A1			B1			B2			C1		
Velocity, m/s	Max	Avg	Min	Max	Avg	Min	Max	Avg	Min	Max	Avg	Min
	4.82	2.06	0.93	4.33	1.99	1.60	4.14	1.75	0.02	5.26	3.71	1.25

The average difference of 1.1 Pa between air pressure outside and inside the tunnel based on the total of 2 min measuring period has been detected. It indirectly supports the assumption of the low positive natural flow existence that was observed during the velocity measurements.

Atmospheric pressure, considering the altitude of the tunnel, is defined as [33]:

$$P = P_0 \cdot \exp\left(-\frac{gMh}{RT}\right) \quad (1)$$

Where P_0 is the standard atmospheric pressure (101,325 Pa), g is the gravitational acceleration (9.81 m/s²), M is the molar mass of air (0.029 kg/mol), h is the altitude of the tunnel (1084 m), R is the universal gas constant (8.314 N·m/(mol·K)), and T is the temperature at the altitude (284.65 K). Thus, the atmospheric pressure during the tests assumed as 88,946 Pa.

2.2 FDS Simulation Setup

2.2.1 Model Settings and Boundary Conditions

Fire Dynamic Simulator (version 6.7.9) is adopted to carry out numerical simulations. The Large Eddy Simulation (LES) mode and the Deardorff turbulence model with the default parameters are used in this study to compute the vortices and fluctuations of relatively large scale in the flow field.

Environmental conditions (ambient temperature and pressure) are set according to the observations (see Sect. 2.1.2).

The ambient in front of the tunnel portal is modelled as a zone where its side and top surfaces are set as "OPEN" to indicate a passive opening to the outside, the bottom surface denotes the ground (road area), and the surface adjacent to the tunnel contains an opening (tunnel gate) connecting the ambient and tunnel spaces. The dynamic pres-

sure of 1.1 Pa is specified here at the "OPEN" boundary to determine the pressure difference between the outside and inside of the tunnel. The "OPEN" property is also applied to the cross-section (parallel to the portal) on the opposite side of the tunnel as it represents the exterior boundary of the computational domain.

The total simulation time is set to 270 s. The jet fans are switched on after 150 s when the stable ventilation mode inside the tunnel is reached in accordance with the applied boundary conditions. During the period between 150 and 210 s, a quasi-stable state of the longitudinal airflow is achieved and the data from 210 to 270 s are considered for the subsequent analysis.

A number of measuring planes, devices and tracing massless particles allow to control the airflow development and record values for velocity, volume flow and pressure. Point gas-phase devices determine air velocity at the locations corresponding to the experimental setup (Fig. 2). At the exact cross-sections, the mean velocity values are defined. Additionally, longitudinal and cross-sectional 2D slices are used to monitor the pattern of flow distribution in terms of pressure and velocity.

2.2.2 The Tunnel

A full-scale numerical model is established according to the project documentation and physical dimensions of the tunnel. A Cartesian coordinate system is assigned along X (length), Y (width), and Z (height) directions. The total length of the tunnel model is 163.2 m, including a 10-meter space in front of the tunnel entrance recreating the ambient (Fig. 2a). The length of the tunnel section is 153.2 m and the distance between the tunnel entry gate and the fan outlets is 50 m. The most distant from the portal a 3-meter long area is used as an extension (additional computational region) to minimize the influence of the model openings while recording the data at the last cross-section (100 m from fan outlets). The importance of the tunnel portal in the model

Fig. 3: The parameters of the cross-section (a) and general view of the tunnel (b)

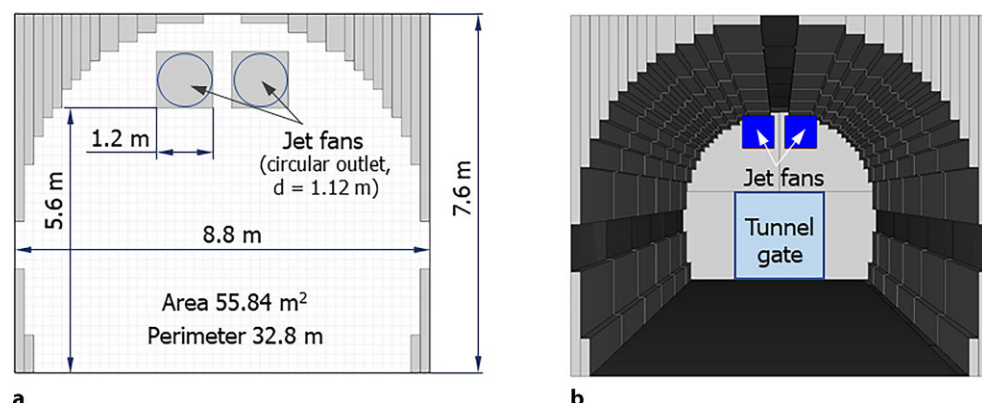


TABLE 4
Details of the meshes adopted in the grid sensitivity analysis

Mesh type	Cell size, m	Total cell number	CPU time, h	Relative difference Volume flow	Velocity
A	0.2×0.1×0.1	5,457,408	91.8	0.006	–
B	0.2×0.2×0.2	1,364,352	13.73	0.032	0.074
C	0.4×0.2×0.2	682,176	5.61	0.044	0.045
D	0.4×0.4×0.4	170,544	1.31	0.105	0.150
E	0.8×0.4×0.4	85,272	0.41	0.360	0.140

is worth noting as it significantly affects the process of air supply from the outside, ensuring a given local resistance. In addition, a straight tunnel model is adopted based on the assumption that the bending radius of a real tunnel is sufficiently large.

The cross-section of the modelled tunnel has a width of 8.8 m and a height of 7.6 m (Fig. 3). The curved ceiling is simplified and constructed using rectangular obstructions. The difference in the cross-sectional areas and wetted perimeters between the real and modelled tunnels is less than 1% (for a mesh with a cell side of 0.2 m) which allows to assume their hydraulic similarity. The material of the tunnel surfaces including walls, ceilings, and floor is set as concrete with a thickness of 0.5 m (other properties specified according to [34]). The tunnel walls are assumed to have a uniform sand roughness height of 0.02 m.

The phenomenon of a “zigzag tunnel wall” in FDS is inevitable when modelling horseshoe-shaped tunnel sections. However, previous studies showed that it is possible to obtain satisfactory results when the numerical grid is fine and the serrated obstruction is small enough [35].

2.2.3 Jet Fans

Two similar tunnel jet fans are modelled in this study. Their geometry is close to the real size (length, width, and height are 3.0, 1.2, and 1.2 m, respectively) and matches the adopted computational mesh. The fans are located under the tunnel ceiling at a height of 5.6 m above the ground (Fig. 3).

The HVAC sub-model is used to simulate the jet fans. It allows air to pass through the fan in a particular direction

with a specified volumetric flow rate across two connected nodes thereby simulating a jet fan’s intake and outlet. The fan flow is directed inside the tunnel (positive value) and has the following attributes added via the HVAC properties: the circular diameter of 1.12 m and the volume flow of 31.4 m³/s (according to Table 1). The fan start up is based on the FDS default ramp up time.

2.2.4 Meshes

The most sensitive numerical parameter in FDS modelling is the mesh (grid cell) size, which affects the accuracy, computational costs and efficiency [36]. A mesh sensitivity analysis is conducted to verify whether the obtained results were influenced by the selection of mesh size during the modelling.

In this study, the computational domain is divided into 6 rectilinear meshes of the same size (27.2×8.8×7.6 m) enabling multiple processor calculations for time efficiency. Five mesh sizes are reviewed in the process. To reduce computing time, an unevenly distributed grid is obtained by stretching the mesh along the X-direction maintaining the recommendation that mesh cells should not possess an aspect ratio larger than 2 to 1. A summary of grid systems and their characteristics for the mesh sensitivity study is given in Table 4.

Volume flow generated by a jet fan and developing longitudinal velocity (mean value for a tunnel cross-section) caused by the pressure difference between the outer and inner spaces of the tunnel are used to assess the sensitivity of the simulation results to the mesh resolution. The dependency of the selected parameters on time using variant

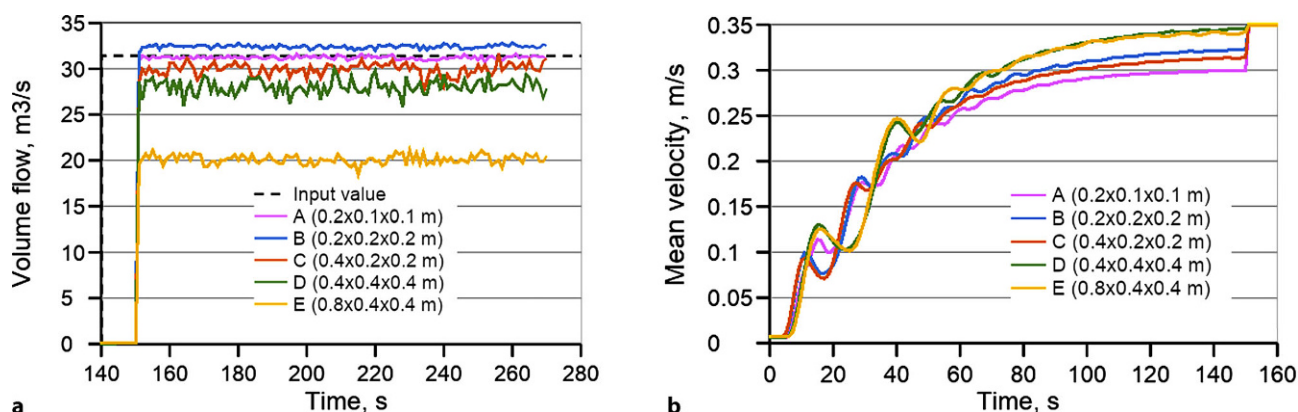


Fig. 4: Influence of grid resolution on volume flow from the jet fan (a) and natural air flow (b)

mesh types is shown in Fig. 4 while the relative difference in average values for a steady period is given in Table 4. The initial input value of fan volume flow and the calculated velocity for the smallest mesh (Type A) are used as reference quantities.

It can be observed that the difference between the mesh types A, B, and C is not sufficient as a deviation under 7.5% could be regarded as acceptable in a CFD simulation. Furthermore, during the mesh sensitivity analysis, it became evident that grid resolution (within the considered range) barely affects the velocities at points located at a distance of 50 m and further from the jet fans. This observation keeps up with the outcomes obtained in the research of multiscale modelling of tunnel ventilation flows [37–39].

On this basis, it can be assumed that mesh type C with a cell size of $0.4 \times 0.2 \times 0.2$ m would be the most suitable option. In this case, the relative difference is less than 5% while the CPU time is about 6% of that required for the finest mesh.

However, mesh resolution heavily impacts the accuracy of results for the areas in the vicinity of jet fans. Thereby, the mesh type B with a cell size of $0.2 \times 0.2 \times 0.2$ m is applied in the model as a balanced solution between efficiency and simulation accuracy. Additionally, the opted mesh resolution corresponds well with the findings in recent publications on tunnel ventilation [40, 41].

2.3 ANSYS Simulation Setup

2.3.1 Model Settings and Boundary Conditions

The Ansys Fluent software (release 2022 R1) is used for numerical modelling. It is assumed that air is an incompressible, isothermal, homogeneous fluid and obeys the law of conservation of mass and momentum.

The simulated boundary conditions followed the actual experimental environment in terms of atmospheric pressure and temperature (see Sect. 2.1.2). Air density and dynamic viscosity are taken as 1.225 kg/m^3 and $1.802 \times 10^{-5} \text{ kg/(m} \cdot \text{s)}$, respectively.

In the computational domain, the planes normal to the fan flow are defined as pressure boundary conditions. The tunnel portal has a square gate (Fig. 1b) representing a surface that is defined as a pressure inlet with a gauge total pressure of 1.1 Pa. The tunnel cross-section from the opposite side of the domain is considered as a pressure outlet with a gauge pressure of 0 Pa. The rest of the planes (tunnel walls, ceiling and floor as well as fan housing) are specified by a non-slip stationary wall boundary condition. The equivalent roughness height of 0.03 m is applied for the tunnel surfaces.

The pair of jet fans are assumed to be represented by fan outlet surfaces for which a pressure jump is defined according to the fan properties (Table 1). The swirl velocity is negligible in the model.

The adopted turbulence model is the standard $k-\varepsilon$ two equation model, and the coupling of pressure and velocity is solved via the SIMPLE algorithm. A transient time model is applied and the total simulation time is 100 s.

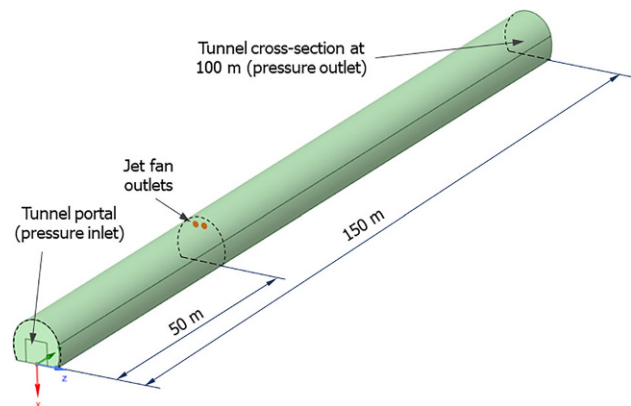


Fig. 5: Overview of the model established in Fluent

2.3.2 The Tunnel

The full-scale Fluent model is established based on the tunnel dimensions. The adopted shape of the cross-section is given in Fig. 2b. The computational domain length corresponds to the experimental scheme where the most distant investigated cross-section is situated at 100 m from the fan outlets (Fig. 5). Thus, the total length of the model is 150 m, and the distance between the tunnel portal and the fans is 50 m.

2.3.3 Meshes

The mesh study is performed to ensure the accuracy of the numerical simulation. Several built-in mesh statistic tools are available in Ansys to quantify the overall grid quality during and after the mesh generation phase. In this research, one of the most commonly used mesh metrics (Orthogonal Quality) is used for the grid evaluation.

The general recommendation on mesh quality states that the minimum orthogonal quality should be more than 0.1 [42]. The “Orthogonal Quality” value for the adopted mesh with the element size of 0.5 m is 0.216, which corresponds to “Good” quality in the mesh metrics spectrum.

An additional mesh size survey is conducted in regard to the jet fan’s performance. The predicted values of centerline velocity generated by a fan are compared to the mathematical model. Namely, for a round jet in the decay phase, the centreline velocity U_x with the increasing distance from the fan outlet follows the formula [43]:

$$U_x = \frac{k U_o D}{x} \quad (2)$$

Where k is a constant (between 3 and 10), U_o is the outlet discharge velocity (31.8 m/s), D is the outlet diameter (1.12 m) and x is the distance from the outlet. Equation 2 is valid for the case when $x = (5 \dots 75) D$.

The comparison of the predicted in Fluent with theoretically calculated values of the centreline velocity for the distance from 15 to 80 m is given in Fig. 6.

Good convergence is observed between the modelled curve and the considered theoretical range while the best agreement is feasible when $k = 4$.

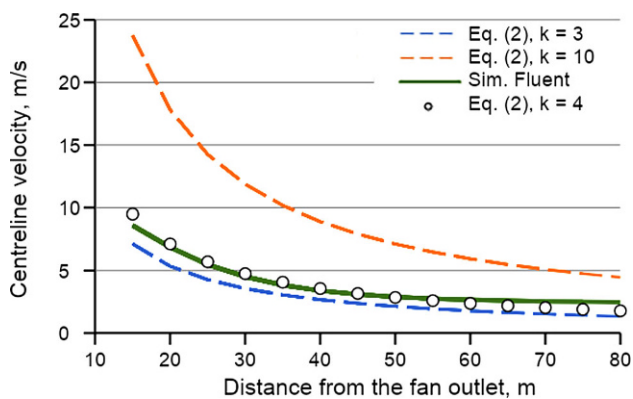


Fig. 6: Dependency of centerline velocities on the distance from the fan outlet

The conducted analysis shows that the adopted grid allows to obtain adequate data in terms of the addressed tasks and thereby is selected for the further numerical study.

2.4 Model Validation

2.4.1 Validation of the FDS Model

The FDS model is validated using data obtained in full-scale tests. A comparison of average velocities along the tunnel length from the experiment and numerical simulation for the randomly chosen measuring point (B2) is given in Fig. 7a. For greater clarity, maximal and minimal measured values and standard deviations (error bars) determined from modelling results are added to the graph. The standard deviation here demonstrates the magnitude of the calculated velocity fluctuations.

The calculated velocity values are significantly close to the measured ones, especially when a dataset's variability (dispersion) is considered.

Good agreement between the test and modelled data is also observed for the upstream locations. The time-dependent velocity profile for two (B1 and C1) of the assessed points at a "–25 m" position is given in Fig. 7b. The simu-

lated velocity curves lie inside the measured range through much of the considered period.

Additionally, the mesh sensitivity analysis described earlier suggests the adequacy of the proposed FDS model providing sufficient reliability in both cases: for naturally developed airflow and mechanical fan ventilation.

2.4.2 Validation of the Fluent Model

The results from the conducted tests are used in the validation process of the Fluent model. The measured velocities are compared with the simulated values along the tunnel length and height. For example, the calculated average velocities for the examined point A1 are presented within the experimentally obtained maximal and minimal bounds in Fig. 8a. Despite some discrepancies, the similarity in the trend and values are clearly visible.

A similar situation is observed when considering the velocity profile along the height of the tunnel (Fig. 8b). The modelled curve for the points in the row (B) at a distance of 30 m from the fan outlets falls in the middle of the measured range and follows its outline.

The discussed findings, coupled with the results of the grid study, lead to the conclusion that the developed Fluent model possesses the required qualities in relation to the current study.

3. Results and Discussion

3.1 Comparison of Experimental and Numerical Data

The development of the flow field regarding its velocity along the tunnel is presented in Fig. 9. These data also contain information about the velocity changes within the assessed tunnel cross-sections. Experimental findings and calculated results are shown together for each measurement point to simplify the comparison process and further analysis. The area bounded by thin lines indicates the longitudinal velocity range between maximal and minimal measured values, while average velocities are shown with a black dashed line. The calculated FDS (round markers)

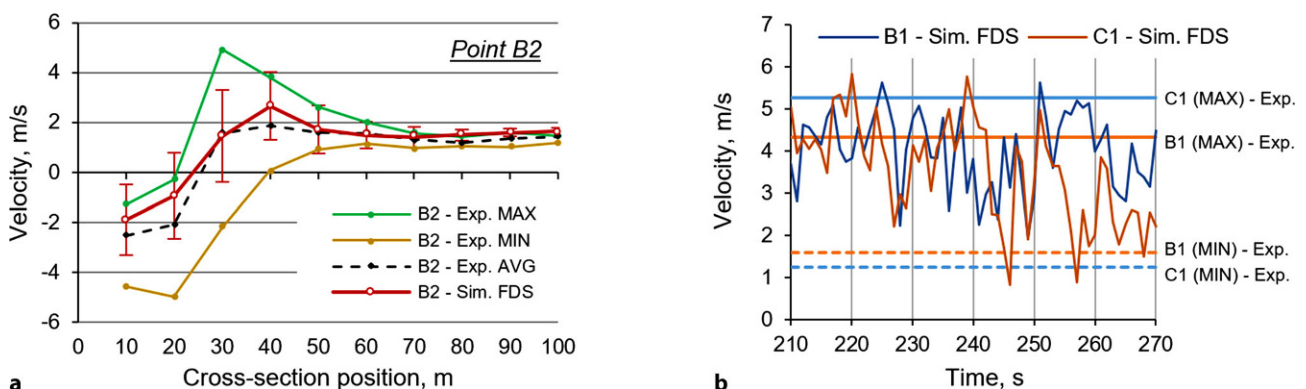


Fig. 7: Comparison of the measured and calculated velocities in the frame of distance (a) and time (b)

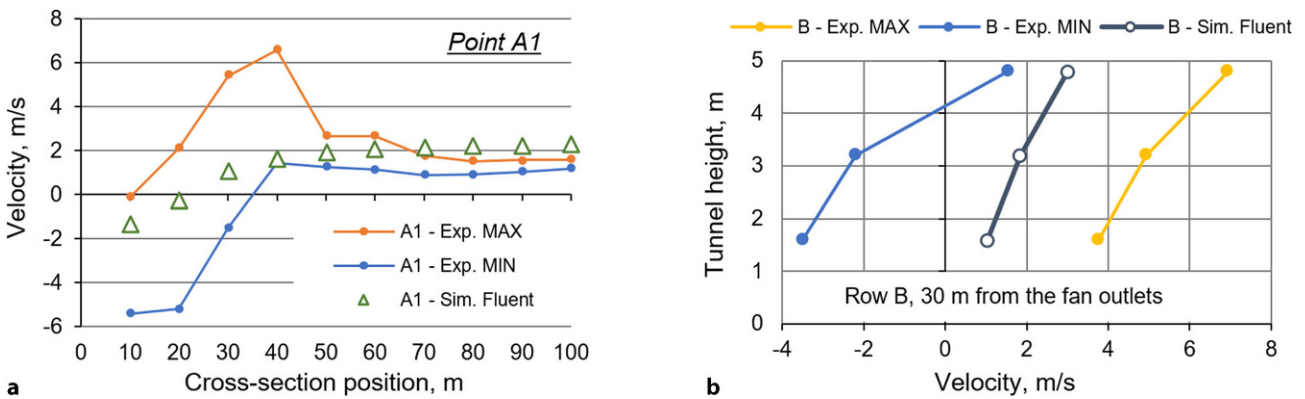


Fig. 8: Comparison of the measured and calculated velocities along the tunnel length (a) and by the tunnel height (a)

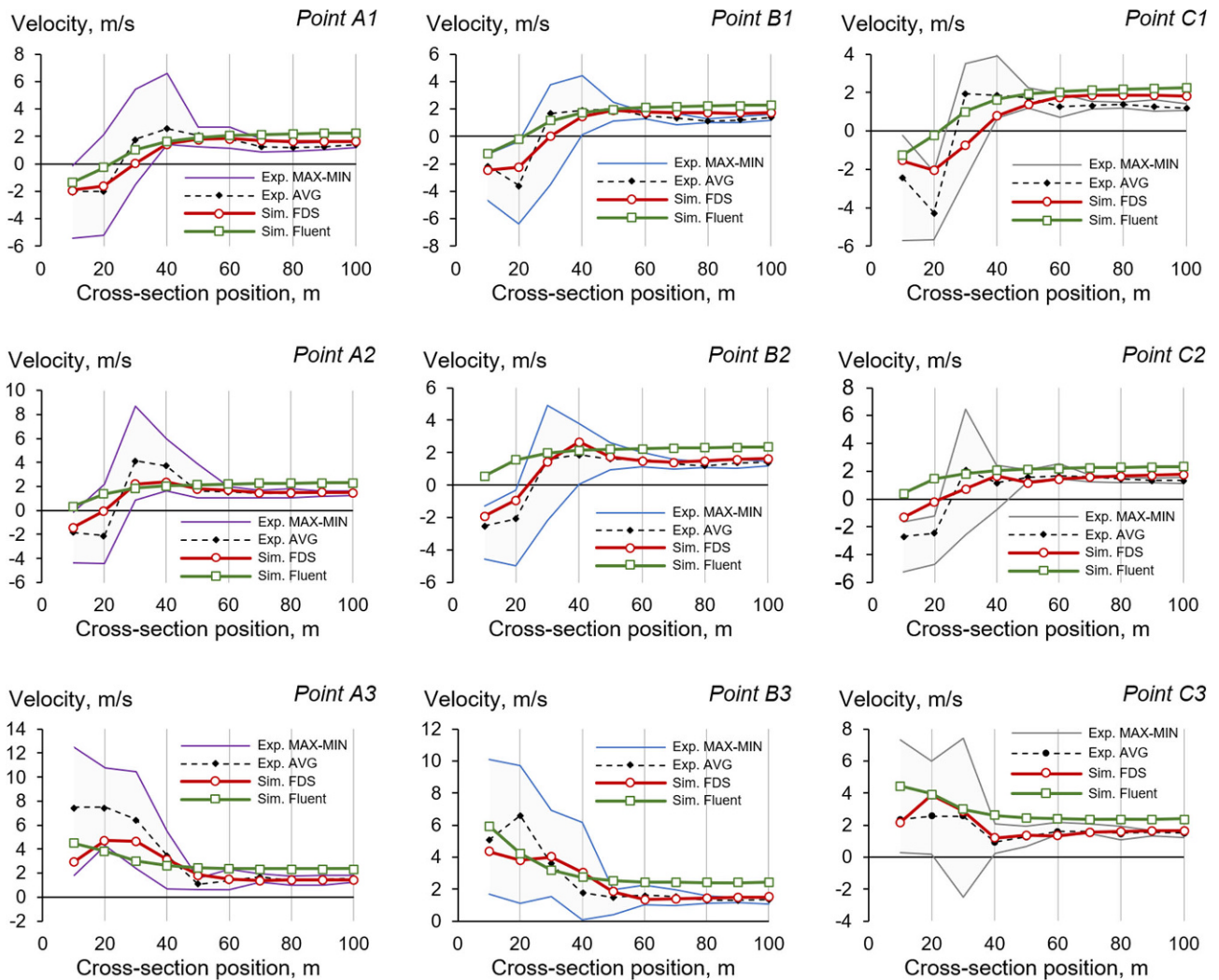


Fig. 9: Comparison of the experimental data and simulation results

and Ansys (square markers) curves are coloured in dark red and green, respectively.

The calculated results indicate good congruence with the field measurements for the majority of the examined spots. Although for some survey points experimental data differ from numerical results, velocity variation trends are

consistent between measurements and simulations. The Fluent and FDS models show acceptable conformity with measured maximum-minimum range, especially at cross-sections from 30 to 100m.

In distant areas (60–100m), the numerical models slightly overestimate the velocity values, wherein the

FDS results are closer to the observations. The adopted straight shape of the tunnel part under study may cause this behaviour as the flow velocities are not additionally affected by occurring local resistance from flow interaction with tunnel walls.

3.2 Backflow Development

The simulation results (FDS and ANSYS) are in good agreement with the field observations regarding the length of the backflow area and its behaviour within the three defined regions (see Sect. 2.1.2). The obtained negative velocities suggest the reverse flow existence within a certain distance from the fan outlets (Fig. 9). It is worth noting that, even when the average value presented in graphs is positive (or negative) for some locations in the fan vicinity, there is a high probability of time-dependent transformation in flow direction due to chaotic changes in pressure and flow velocity.

The same situation concerns the highlighted by font styles quantities in Table 2, where, despite the positive maximum, average, and minimum values for several locations the negative flow was observed (e.g. points A1 at 40 m, A2 at 30 m, etc.). For example, at point B1 at a distance

of 40 m from the fan outlets, we see a minimal velocity of 0.13 m/s and the bold font marking of the reverse flow presence. It can be assumed that the “wavy” flow development affected by turbulence causes this behaviour. The FDS simulation results support this assumption as velocity fluctuations of a changing magnitude and direction are predicted during a quasi-stable flow state (Fig. 10a). The same applies to points (e.g., A1 at 10 m, B1 at 20 m, etc.) with negative measured values where the positive air flow was observed (Fig. 10b).

The obtained results also show the dependency of the backflow existence and its intensity on the height and distance from the fan outlets. Two layers with opposite flow directions can be distinguished at the velocity profile (Fig. 11). The presented flow fields are obtained for the middle tunnel longitudinal section after the air flow reached its quasi-stable state.

It can be assumed that a stable backflow zone occurs within a 30-meter distance from the fan outlets. However, local airstreams of a negative direction may occasionally appear in the region up to 50 m.

Similar flow patterns show a velocity distribution in the vicinity of the fans. The moderate difference in terms of velocity magnitude may be caused by the difference in the applied turbulence models (LES and $k-\epsilon$ for FDS and Fluent,

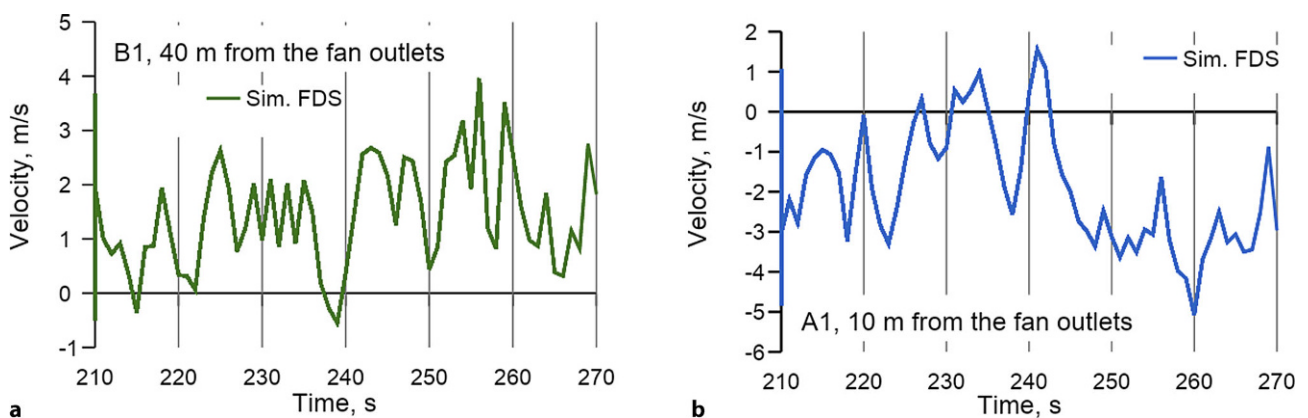
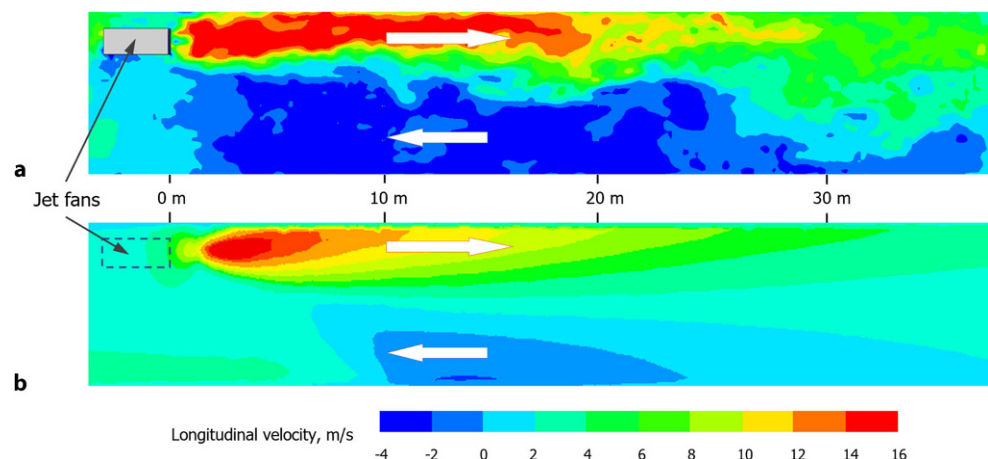


Fig. 10: Velocity development in time at points B1 (a) and A1 (b)

Fig. 11: Velocity profile for the tunnel longitudinal section modelled by FDS (a) and Fluent (b)



respectively) as well as grid resolution (the FDS model has a finer mesh).

4. Conclusions

In this study, two CFD models were developed using Fire Dynamic Simulator and Ansys Fluent for the investigation of the ventilation issues regarding the backflow development in the tunnel of the "Zentrum am Berg" facility. A full-scale experiment for the evaluation of the ventilation conditions in the western railway tunnel was carried out. The results obtained were used for the assessment of the numerical models by comparing the predicted velocities with their measured values. The main results are as follows:

- The simulated with both CFD packages velocity variation trends are in good agreement with field measurements.
- Predictably, the greatest discrepancies in the data are observed in areas close to the fans due to high turbulence and the backflow presence.
- Good convergence of results is observed for the quasi-stable state of the airflow at distances from 30 to 100 m though the simulated velocities are slightly overestimated at the more distant cross-sections. In this area, the FDS results were closer to the experimental data.
- The simulated backflow development corresponds to that observed concerning the three specified regions (initial, transitional and developed) with distinctive flow structures.
- The observed spontaneous changes in flow direction for points with a prevailed flow direction (positive or negative) were confirmed by the FDS-simulated velocity curves.

The comparative analysis of two numerical models shows their applicability in the backflow study. Depending on the tasks to be solved further adjustment of the numerical models could improve the congruence between the predicted and experimental results providing reliable and efficient solutions.

Funding. Open access funding provided by Montanuniversität Leoben.

Open Access This article is licensed under a Creative Commons Attribution 4.0 International License, which permits use, sharing, adaptation, distribution and reproduction in any medium or format, as long as you give appropriate credit to the original author(s) and the source, provide a link to the Creative Commons licence, and indicate if changes were made. The images or other third party material in this article are included in the article's Creative Commons licence, unless indicated otherwise in a credit line to the material. If material is not included in the article's Creative Commons licence and your intended use is not permitted by statutory regulation or exceeds the permitted use, you will need to obtain permission directly from the copyright holder. To view a copy of this licence, visit <http://creativecommons.org/licenses/by/4.0/>.

References

1. Ingason, H., Li, Y.Z., Lönnemark, A.: Tunnel fire dynamics. Springer, New York (2015)
2. Chang, X., Chai, J., Liu, Z., Qin, Y., Xu, Z.: Comparison of ventilation methods used during tunnel construction. *Eng. Appl. Comput. Fluid Mech.* **14**(1), 107–121 (2020). <https://doi.org/10.1080/19942060.2019.1686427>
3. Chang, X., Chai, J., Luo, J., Qin, Y., Xu, Z., Cao, J.: Tunnel ventilation during construction and diffusion of hazardous gases studied by numerical simulations. *Build Environ* **177**, 106902 (2020). <https://doi.org/10.1016/j.buildenv.2020.106902>
4. Wang, H., Jiang, Z., Zhang, G., Zeng, F.: Parameter analysis of jet tunnel ventilation for long distance construction tunnels at high altitude. *J. Wind. Eng. Ind. Aerodyn.* **228**, 105128 (2022). <https://doi.org/10.1016/j.jweia.2022.105128>
5. Król, A., Król, M., Koper, P., Wrona, P.: Numerical modeling of air velocity distribution in a road tunnel with a longitudinal ventilation system. *Tunn. Undergr. Space Technol.* **91**, 103003 (2019). <https://doi.org/10.1016/j.tust.2019.103003>
6. Zhao, S., Xue, P., Xie, J., Wang, Y., Jiang, Z., Liu, J.: Optimal pitch angle of jet fans based on air age evaluation for highway tunnel ventilation. *J. Wind. Eng. Ind. Aerodyn.* **228**, 105088 (2022). <https://doi.org/10.1016/j.jweia.2022.105088>
7. Wang, M., Guo, X., Yu, L., Zhang, Y., Tian, Y.: Experimental and numerical studies on the smoke extraction strategies by longitudinal ventilation with shafts during tunnel fire. *Tunn. Undergr. Space Technol.* **116**, 104030 (2021). <https://doi.org/10.1016/j.tust.2021.104030>
8. Nely, G., Sivelina, D., Petko, T.: Analysis of the capabilities of software products to simulate the behavior of dynamic fluid flows. *IOP Conf. Ser.: Mater. Sci. Eng.* **1031**(1), 12079 (2021). <https://doi.org/10.1088/1757-899x/1031/1/012079>
9. Abrahamson, J.: Ansys Fluent Theory Guide. Release 2022 R1. ANSYS, Canonsburg (2022)
10. Król, A., Król, M.: Transient analyses and energy balance of air flow in road tunnels. *Energies* **11**(7), 1759 (2018). <https://doi.org/10.3390/en11071759>
11. Chen, T., Zhou, D., Lu, Z., Li, Y., Xu, Z., Wang, B., Fan, C.: Study of the applicability and optimal arrangement of alternative jet fans in curved road tunnel complexes. *Tunn. Undergr. Space Technol.* **108**, 103721 (2021). <https://doi.org/10.1016/j.tust.2020.103721>
12. Chen, T., Li, Y., Xu, Z., Kong, J., Liang, Y., Wang, B., Fan, C.: Study of the optimal pitch angle of jet fans in road tunnels based on turbulent jet theory and numerical simulation. *Build. Environ.* **165**, 106390 (2019). <https://doi.org/10.1016/j.buildenv.2019.106390>
13. Liu, Z., Wang, X., Cheng, Z., Sun, R., Zhang, A.: Simulation of construction ventilation in deep diversion tunnels using Euler-Lagrange method. *Comput. Fluids* **105**, 28–38 (2014). <https://doi.org/10.1016/j.compfluid.2014.09.016>
14. Myrvang, T., Khawaja, H.: Validation of air ventilation in tunnels, using experiments and computational fluid dynamics. *IJM* **12**(3), 295–311 (2018). <https://doi.org/10.21152/1750-9548.12.3.295>
15. Musto, M., Rotondo, G.: Numerical comparison of performance between traditional and alternative jet fans in tiled tunnel in emergency ventilation. *Tunn. Undergr. Space Technol.* **42**, 52–58 (2014). <https://doi.org/10.1016/j.tust.2014.02.003>
16. McGrattan, K., Hostikka, S., Floyd, J., McDermott, R., Vanella, M.: Fire Dynamics Simulator User's Guide, 6th edn. NIST, Gaithersburg (2022)
17. McGrattan, K., Hostikka, S., Floyd, J., McDermott, R., Vanella, M.: Fire Dynamics Simulator Technical Reference Guide. Volume 1: Mathematical Model, 6th edn. NIST, Gaithersburg (2022)
18. McGrattan, K., Hostikka, S., Floyd, J., McDermott, R., Vanella, M.: Fire Dynamics Simulator Technical Reference Guide. Volume 2: Verification, 6th edn. NIST, Gaithersburg (2022)
19. McGrattan, K., Hostikka, S., Floyd, J., McDermott, R., Vanella, M.: Fire Dynamics Simulator Technical Reference Guide. Volume 3: Validation, 6th edn. NIST, Gaithersburg (2022)
20. Yuan, S., Sun, X., Liu, S., Li, Y., Du, P.: Effectiveness of cluster-based inductive ventilation system in railway tunnels: Case study using full-scale experiment and fire dynamic simulation. *Case Stud. Therm. Eng.* **34**, 102045 (2022). <https://doi.org/10.1016/j.csite.2022.102045>
21. Weisenpacher, P., Valasek, L.: Computer simulation of airflows generated by jet fans in real road tunnel by parallel version of FDS 6. *Int. J. Vent.* **20**(1), 20–33 (2019). <https://doi.org/10.1080/14733315.2019.1698164>

22. Sun, J., Tang, Z., Fang, Z., Beji, T., Merci, B.: Flow fields induced by longitudinal ventilation and water spray system in reduced-scale tunnel fires. *Tunn. Undergr. Space Technol.* **104**, 103543 (2020). <https://doi.org/10.1016/j.tust.2020.103543>
23. Weng, M., Obadi, I., Wang, F., Liu, F., Liao, C.: Optimal distance between jet fans used to extinguish metropolitan tunnel fires: A case study using fire dynamic simulator modeling. *Tunn. Undergr. Space Technol.* **95**, 103116 (2020). <https://doi.org/10.1016/j.tust.2019.103116>
24. Ang, C.D., Rein, G., Peiro, J., Harrison, R.: Simulating longitudinal ventilation flows in long tunnels: Comparison of full CFD and multi-scale modelling approaches in FDS6. *Tunn. Undergr. Space Technol.* **52**, 119–126 (2016). <https://doi.org/10.1016/j.tust.2015.11.003>
25. Beard, A., Carvel, R.: *The handbook of tunnel fire safety*, 2nd edn. ICE, London (2012)
26. Cai, X., Nie, W., Yin, S., Liu, Q., Hua, Y., Guo, L., Cheng, L., Ma, Q.: An assessment of the dust suppression performance of a hybrid ventilation system during the tunnel excavation process: Numerical simulation. *Process. Saf. Environ. Prot.* **152**, 304–317 (2021). <https://doi.org/10.1016/j.psep.2021.06.007>
27. Sturm, P.-J., Bacher, M., Beyer, M., Schmölzer: The influence of pressure gradients on ventilation design—Special focus on upgrading long tunnels. In: *Tunnel Safety and Ventilation*, pp. 90–99. Verlag der Technischen Universität Graz, Graz (2012)
28. Nan, C., Ma, J., Luo, Z., Zheng, S., Wang, Z.: Numerical study on the mean velocity distribution law of air backflow and the effective interaction length of airflow in forced ventilated tunnels. *Tunn. Undergr. Space Technol.* **46**, 104–110 (2015). <https://doi.org/10.1016/j.tust.2014.11.006>
29. Yang, S., Ai, Z., Zhang, C., Dong, S., Ouyang, X., Liu, R., Zhang, P.: Study on optimization of tunnel ventilation flow field in long tunnel based on CFD computer simulation technology. *Sustainability* **14**(18), 11486 (2022). <https://doi.org/10.3390/su141811486>
30. Mutama, K.R., Hall, A.E.: Theoretical analysis of jet fan performance using momentum and energy considerations. In: *8th US Mine Ventilation Symposium*, pp. 469–476. (1999)
31. Patsekha, A., Galler, R.: Concept development for evaluating the impact of operating inside road tunnel fans on the airflow structure in their vicinity. In: *Disaster Research Days 2021. Disaster Competence Network Austria*, pp. 19–20. (2021)
32. Tavoularis, S.: *Measurement in Fluid Mechanics*. Cambridge University Press, Cambridge (2005)
33. Barometric Formula. <https://math24.net/barometric-formula.html>, Accessed 30 Sept 2022
34. Hurlley, M.J., Gottuk, D., Hall, J.R., Harada, K., Kuligowski, E., Puchovsky, M., Torero, J., Watts, J.M., Wieczorek, C.: *SFPE Handbook of Fire Protection Engineering*. Springer, New York (2016)
35. Xu, Z., Zhou, D., Tao, H., Zhang, X., Hu, W.: Investigation of critical velocity in curved tunnel under the effects of different fire locations and turning radiuses. *Tunn. Undergr. Space Technol.* **126**, 104553 (2022). <https://doi.org/10.1016/j.tust.2022.104553>
36. Weng, M., Lu, X., Liu, F., Shi, X., Yu, L.: Prediction of backlayering length and critical velocity in metro tunnel fires. *Tunn. Undergr. Space Technol.* **47**, 64–72 (2015). <https://doi.org/10.1016/j.tust.2014.12.010>
37. Colella, F.: *Multiscale analysis of tunnel ventilation flows and fires*. PhD Thesis, Politecnico di Torino, Dipartimento di Energetica (2010)
38. Álvarez-Coedo, D., Ayala, P., Cantizano, A., Węgrzyński, W.: A coupled hybrid numerical study of tunnel longitudinal ventilation under fire conditions. *Case Stud. Therm. Eng.* **36**, 102202 (2022). <https://doi.org/10.1016/j.csite.2022.102202>
39. Xu, C., Li, Y., Feng, X., Li, J.: Multi-scale coupling analysis of partial transverse ventilation system in an underground road tunnel. *Procedia Eng.* **211**, 837–843 (2018). <https://doi.org/10.1016/j.proeng.2017.12.082>
40. Król, A., Król, M.: Numerical investigation on fire accident and evacuation in a urban tunnel for different traffic conditions. *Tunn. Undergr. Space Technol.* **109**, 103751 (2021). <https://doi.org/10.1016/j.tust.2020.103751>
41. Yang, P., Shi, C., Gong, Z., Tan, X.: Numerical study on water curtain system for fire evacuation in a long and narrow tunnel under construction. *Tunn. Undergr. Space Technol.* **83**, 195–219 (2019). <https://doi.org/10.1016/j.tust.2018.10.005>
42. Fatchurrohman, N., Chia, S.T.: Performance of hybrid nano-micro reinforced mg metal matrix composites brake calliper: simulation approach. *IOP Conf. Ser.: Mater. Sci. Eng.* **257**, 12060 (2017). <https://doi.org/10.1088/1757-899X/257/1/012060>
43. Mutama, K.R.: *Wind tunnel investigation of jet fan aerodynamics*. PhD Thesis, University of British Columbia (1995)

Publisher's Note. Springer Nature remains neutral with regard to jurisdictional claims in published maps and institutional affiliations.